NASA Technical Paper 2271

1984

Mean Excitation Energies for Stopping Powers in Various Materials Using Local Plasma Oscillator Strengths

John W. Wilson
Langley Research Center
Hampton, Virginia

Y. J. Xu
Old Dominion University
Norfolk, Virginia

Efstathios Kamaratos
and C. K. Chang
Christopher Newport College
Newport News, Virginia

National Aeronautics
and Space Administration

Scientific and Technical Information Branch

SUMMARY

The basic model of Lindhard and Scharff, known as the local plasma model, is utilized to study the effects on stopping power of the chemical and physical state of the medium. Unlike previous work with the local plasma model, in which individual electron shifts in the plasma frequency were estimated empirically, the Pines correction derived for a degenerate Fermi gas is shown herein to provide a reasonable estimate, even on the atomic scale. Thus, the model is moved to a complete theoretical base requiring no empirical adjustments, as characteristic of past applications. The principal remaining error is in the overestimation of the low-energy absorption properties that are characteristic of the plasma model in the region of the atomic discrete spectrum, although higher-energy phenomena are accurately represented, and even excitation-to-ionization ratios are given to fair accuracy. Mean excitation energies for covalent-bonded gases and solids, for ionic gases and crystals, and for metals are calculated using first-order models of the bonded states, for which reasonable agreement with the recently evaluated data of Seltzer and Berger is obtained. Hence, the methods described herein allow reasonable estimates of mean excitation energy for any physical-chemical combination of material media for stopping-power applications.

INTRODUCTION

The impact of energetic ions with atoms and molecules is a fundamental physical phenomenon with numerous applications in areas such as astrophysics, medical physics, high-power lasers, and plasma fusion devices, and is of special interest for radiation protection of people and materials in space. Most of what is known in modern physics is ultimately related to observations of charged-particle impact phenomena, by which particle character is studied, starting with the early works of Rutherford using radioactive sources. To advance our knowledge of such processes is both timely and technologically important. The historical context in which present theoretical developments are to be understood is discussed in the following section.

HISTORICAL PERSPECTIVE

It was recognized early in the classical treatment of charged particle slowing down that the free-electron, long-range Coulomb interaction leads to divergencies in the energy-loss rate. These divergencies indicate that there is a need for a long-range saturation effect. The saturation in gases was discussed by Bohr (ref. 1) in terms of Ehrenfest's principle. Bohr proposed that the saturation in gases is caused by the bonding of the electrons. To effect energy transfer, the interaction time $\tau = b/v$ (where b is the impact parameter and v the ion velocity) must be short compared with the oscillating period of the bonded electron. (A list of symbols and abbreviations used in this paper appears after the references.) Hence, the adiabatic long-range collisions provide the necessary saturation, and an upper limit is established for the effective impact parameters. Most of our modern understanding stems

from Bethe's detailed quantum theory (ref. 2) based on the Born approximation. Stopping power for gaseous media with this approximation is given by

$$S = \frac{4\pi n Z_1^2 Z_2 e^4}{mv^2} \left\{ \ln \left[\frac{2mv^2}{(1 - \beta^2) I_2} \right] - \beta^2 - \frac{C}{Z_2} \right\} \tag{1}$$

where Z_1 is the projectile charge, n is the number of targets per unit volume, Z_2 is the number of electrons per target, m is the electron mass, v is the projectile velocity, $\beta = v/c$, c is the velocity of light, C is the velocity-dependent shell-correction term (ref. 3), and I_2 is the mean excitation energy given by solving

$$Z_2 \ln I_2 = \sum_n f_n \ln E_n \tag{2}$$

where f_n is the electric dipole oscillator strength of the target and E_n is the corresponding excitation energy. The sum in equation (2) includes discrete and continuum levels. Empirically, it was observed that molecular stopping power is reasonably approximated by the sum of the corresponding empirically derived "atomic" stopping powers (ref. 4). Equations (1) and (2) imply

$$Z \ln I = \sum_j n_j Z_j \ln I_j \tag{3}$$

where Z and I pertain to the molecule, Z_j and I_j are the corresponding atomic values, and n_j represents the stoichiometric coefficients. This additivity rule, given by equation (3), is called Bragg's rule.

Sources of deviations from Bragg's additivity rule for molecules and the condensed phase are discussed by Platzman (ref. 5). Aside from shifts in excitation energies and adjustments in line strengths as a result of molecular bonding, new terms in the stopping power are caused by the coupling of vibrational and rotational modes. Additionally, in the condensed phase, some discrete transitions are moved into the continuum, and collective modes among valence electrons in adjacent atoms produce new terms to be dealt with in the absorption spectrum. Platzman proposed that the experimentally observed additivity rule may not show that molecular stopping power is the sum of atomic processes but rather that it demonstrates that molecular bond shifts for covalent-bonded molecules are relatively independent of the molecular combination. On the basis of such arguments, Platzman suggested ionic-bonded substances as the ones which should be studied as a rigid test of the additivity rule because of the radical difference in bonding type. He further estimated that ionic-bond shifts could change the stopping power by as much as 50 percent.

Among the early indicators of the violation of the Bragg rule was the calculation of 15 eV for the mean excitation energy of atomic hydrogen (using eq. (2) with the exactly known oscillator strengths and excitation levels) compared with a rather firmly established experimental value for molecular hydrogen of about 18 eV. Since accurate values of atomic mean excitation energies have been calculated for numerous

elements by Inokuti and co-workers (refs. 6 to 8) for the purpose of evaluating chemical bonding effects in molecules, empirical values have been substantially perturbed by effects of the chemical bonds. Although the mean excitation energy for gas molecules could be evaluated in principle from equation (2), the lack of knowledge of the excitation levels and corresponding oscillator strengths is the main hindrance.

It was suggested by Dalgarno (ref. 9) that the oscillator strength distributions could be determined empirically from the photoabsorption spectra (aside from experimental uncertainty). Much of these data are obtained by energy-loss experiments by electron impact scattering at forward angles. Values of mean excitation energy for a number of simple molecules have in this way been estimated, and have demonstrated the shift in atomic values caused by chemical bonding (refs. 10 and 11).

Theoretical calculation of mean excitation energies is hindered by the difficulty of solving for the complete excitation spectrum of complex quantum systems. Dalgarno was able to simplify the calculation by introducing a generalized function, which is related to the excitation spectrum as follows:

$$F_D(\omega) = \sum_n \frac{f_n}{E_n + \omega} \tag{4}$$

However, this function can be evaluated without explicitly forming the indicated sum. Thus, Dalgarno (ref. 12) was able to reduce equation (4) to

$$F_D(\omega) = \frac{2}{3}\left(\vec{X}, \sum_{i=1}^{Z_2} \nabla_i \psi_o\right) \tag{5}$$

with

$$(H - E_o + \omega)\vec{X} + \sum_{i=1}^{Z_2} \vec{r}_i \psi_o = 0 \tag{6}$$

where ψ_o is the ground-state wave function, E_o is the corresponding energy, ω is an energy eigenvalue, and $\vec{X}$ is the corresponding eigenvector. Chan and Dalgarno (ref. 13) calculated I as 42 eV for helium and Kamikawai et al. (ref. 14) calculated 18.2 eV for molecular hydrogen by the same method. These values are in excellent agreement with experiments.

Simultaneous with the development of the microscopic theory of stopping power was the macroscopic electrodynamic description of energy loss as required for the description of the long-range part of the interaction in condensed phase. This is because the interaction is simultaneous among many constituents. The slowing down is through the force exerted on the passing particle by the electric field induced in

the medium by the passage (ref. 15). It is customary to assume that the electric displacement vector is linearly related to the time-varying electric field as

$$\vec{D}(t) = \vec{E}(t) + \int_0^t g(\tau)\, \vec{E}(t - \tau)\, d\tau \tag{7}$$

for which the dielectric constant is

$$\varepsilon(\omega) = 1 + \int_0^\infty g(\tau) \exp(i\omega\tau)\, d\tau \tag{8}$$

The short-range collisions are still treated by Bethe theory with the result for total stopping power (see ref. 16 for details) of

$$S = \frac{4\pi n Z_1^2 Z_2 e^4}{mv^2} \left\{ \ln\left[\frac{2mv^2}{(1 - \beta^2) I_2} \right] - \beta^2 - \frac{\delta}{2} \right\} \tag{9}$$

where δ is a density-effect correction applicable at high energies $\left(\beta^2 > 1/\varepsilon(0)\right)$. Also,

$$Z_2 \ln I_2 = \frac{m}{2\pi^2 n e^2} \int_0^\infty \omega\, \mathrm{Im}\left[\frac{-1}{\varepsilon(\omega)} \right] \ln(\hbar\omega)\, d\omega \tag{10}$$

where $\mathrm{Im}(Z)$ denotes the imaginary part of Z. A result of dispersion theory is

$$\frac{m}{2\pi^2 n e^2} \omega\, \mathrm{Im}[\varepsilon(\omega)] = f(\omega) \tag{11}$$

where $f(\omega)$ is the dipole oscillator strength per unit cell of the medium, so that

$$Z_2 \ln I_2 = \int_0^\infty \frac{f(\omega)}{|\varepsilon(\omega)|^2} \ln(\hbar\omega)\, d\omega \tag{12}$$

which reduces to the usual Bethe expression (eq. (2)) in a sparse gas for which $\varepsilon(\omega) \approx 1$.

If the long-range saturation effect is in terms of adiabatic limits for a gas and in terms of the medium polarization response for condensed dielectrics, the saturation effect for a free-electron gas is related to the tendency of a neutral

plasma to screen a local charge imbalance at large distances (ref. 17). The dielectric function of a free-electron gas is derived by Lindhard (ref. 18) and applied to the stopping-power problem for a classical electron gas and for the interaction-free Sommerfeld electron gas model. For a free-electron gas at rest, Lindhard arrives at the equation

$$S = \frac{4\pi Z_1^2 e^4 \rho}{mv^2} \ln\left(\frac{2mv^2}{\hbar\omega_p}\right) \tag{13}$$

where ρ is the electron density and ω_p is the classical plasma frequency given by

$$\omega_p^2 = \frac{4\pi e^2}{m} \rho \tag{14}$$

Strictly speaking, equation (13) applies only when the electron gas is at rest, but it also applies in the limit of high projectile velocity compared with the average motion of the electrons.

A discovery which paralleled the Lindhard investigations was made by Bohm and Pines (refs. 19 to 21), in which collective long-range interactions in a quantum electron gas were separated from individual electron motion through a canonical transformation, after which the normal coordinates of collective oscillation appear. This separation of the Hamiltonian into collective and individual electron motion is accomplished because of the effective screening of the Coulomb fields of individual electrons for distances greater than the screening distance λ_c. For collective motion to give a major contribution to the Hamiltonian, the individual electron wavelength must be greater than λ_c. Bohm and Pines (ref. 21) found the average collective plasma frequency to be

$$\langle\omega\rangle = \left[1 + \frac{3}{2}\frac{\chi^2}{\lambda_s}\left(1 + \frac{3}{10}\chi^2\right)\right]\omega_p \tag{15}$$

where λ_s is the average electron separation and χ is the ratio of the average electron wavelength to the screening distance. Pines (ref. 22) suggests that the screening parameter χ should be chosen to minimize the electron long-range correlation energy (that is, the electronic Coulomb energy), which, for plane-wave states appropriate to their degenerate electron gas, is given by

$$E_{lr,corr} = \frac{0.866\chi^3}{\lambda_s^{1.5}} - \frac{0.458\chi^2}{\lambda_s} + \frac{0.019\chi^4}{\lambda_s} \tag{16}$$

Pines (ref. 22) derived the stopping power in this degenerate electron gas and showed that the usual classical plasma frequency ω_p is replaced by $\langle\omega\rangle$, which includes corrections for individual electron motion.

A rather bold suggestion was made by Lindhard and Scharff (ref. 23) that equation (13) could be applied on the atomic scale if the appropriate average over the atomic electron density was made. They further suggested that the effects of individual bonding of the electrons in their atomic orbitals could be incorporated through the added factor $\gamma \approx \sqrt{2}$ as

$$S = \frac{4\pi e^4 Z_1^2 n}{mv^2} \int d^e r \; \rho(\vec{r}) \; \ln\left(\frac{2mv^2}{\gamma\hbar\omega_p}\right) \tag{17}$$

From equation (17), the mean excitation energy is given by

$$Z_2 \ln I_2 = \int d^3 r \; \rho(\vec{r}) \; \ln(\gamma\hbar\omega_p) \tag{18}$$

Lindhard and Scharff estimated the mean excitation energy for atomic Hg as 768 eV compared with ≈800 eV from experiments. For He, they got 37 eV compared with 35 eV from quoted experiments. They further approximated molecular hydrogen by taking the effective charge to be $Z = 1.2$ and obtained 16 eV.

Following this initial success of treating atoms as localized electron plasmas, Lindhard and Winther (ref. 24) extended equation (17) by using the more general velocity-dependent dielectric function derived by Lindhard (ref. 18), and demonstrated the ability of the Lindhard theory to predict tight bonding corrections of similar character to those of Walske (ref. 25) in connection with the Bethe theory.

Chu and Powers (ref. 26) made extensive use of the work of Lindhard and Scharff (ref. 23) to demonstrate Z_2 oscillations in the mean excitation energy. This work gave rise to corresponding Z_2 oscillations in stopping power from which periodic variations are associated with the atomic shell structure (ref. 26). The more detailed calculations of Rousseau et al. (ref. 27) utilized the velocity-dependent Lindhard-Winther theory (ref. 24) and Bonderup's simplified form of the Lindhard theory (ref. 28) and show good agreement with 2-MeV alpha-particle stopping-power data (ref. 29). Throughout these efforts, the parameter γ is taken as the square root of 2, as suggested by Lindhard and Scharff (ref. 23).

Chu et al. (ref. 30), using the theory of Lindhard and Winther in which individual electron corrections to the local collective excitation were treated empirically by taking γ as an adjustable parameter, evaluated the aggregation effects for condensed noble gases and metals. The condensed-gas calculations determined electron densities according to atomic Hartree-Fock densities, including overlap from the nearest neighbors in the condensed phase. Metallic wave functions were taken from the muffin-tin calculations of Moruzzi et al. (ref. 31). In most cases, γ was in the range from 1.2 to 1.3. (See ref. 32.)

As noted by Dehmer et al. (ref. 6) equation (18) may be rewritten as

$$Z_2 \ln I_2 = \int dw \; [\int d^3 r \; \delta(\omega - \gamma\omega_p) \; \rho(r)] \; \ln(\hbar\omega) \tag{19}$$

from which can be obtained

$$f(\omega) = \int d^3r \, \delta(\omega - \gamma\omega_p) \, \rho(r) \tag{20}$$

where $\delta(x)$ is the delta function. It is seen from equation (20) that, in the local plasma approximation, the volume of plasma with cutoff frequency $\gamma\omega_p = \omega$ approximates the total oscillator strength of the system at frequency ω. No exact equivalence is implied between the oscillator frequency distribution given by equation (20) and the oscillator frequency distribution of a quantum system. (This is true because eq. (20) exhibits a continuous spectrum, although quantum systems generally exhibit a series of poles associated with the discrete quantum levels as well as a continuum at higher frequencies.) Some insight may be gained by comparing dispersion relations for atomic systems with those for a related plasma. The dispersion relation for a classical plasma is given by the dielectric constant $\varepsilon(\omega)$ as

$$\varepsilon(\omega) = 1 - \frac{\omega_p^2}{\omega^2} \tag{21}$$

where ω_p is the usual plasma frequency and equation (21) results from the plasma conductivity (ref. 33). Indeed, the same pole appears in metals as the result of the conduction electrons from which the characteristic optical properties of metals derive (refs. 33 and 34). The more general dispersion relation, derived from equations (8) and (11), is

$$\varepsilon(\omega) = 1 - \frac{4\pi Z_2 e^2}{m} P \int_0^\infty \frac{f(x)}{x^2 - \omega^2} dx \tag{22}$$

where P denotes the principal value at the singularity. In atomic systems, the oscillator strengths are broadly separated in frequencies according to shells; the outer shells appear at the lowest frequencies, and the innermost shell appears at the highest frequencies. The lack of oscillator strength at frequencies between shells results in large gaps in the spectrum. Let ω be a frequency in the broad gap between two successive shells - the first centered at ω_1 and the second at ω_2. Then the dispersion relation (eq. (22)) becomes

$$\varepsilon(\omega) \approx 1 - \frac{\omega_{p,1}^2}{\omega^2} \tag{23}$$

where

$$\omega_{p,1}^2 \approx \frac{4\pi e^2 Z_2}{m} \int_0^{\omega_1} f(x)\, dx \tag{24}$$

so that $\omega_{p,1}$ is the plasma frequency associated with the electrons of the outermost shell. Although equations (23) and (24) provide motivation for using the local plasma approximation (eq. (20)), there is plenty of room for a more complete understanding as to why the model works as well as it does in practical calculations (ref. 35).

In previous investigations, we considered the use of the local plasma model to evaluate molecular bonding effects on the mean excitation energy of molecules of covalently bonded hydrogen and carbon (ref. 35) as well as ionic crystals and gases (ref. 36), in which quite sensible corrections to the usual Bragg rule were obtained. The chemical bond shifts were unambiguously defined in terms of atomic integrals and molecular parameters. In the usual implementation of the local plasma model (eq. (18)), γ corrects for a shift in the local plasma frequency caused by individual electron effects. Lindhard and Scharff (ref. 23) suggest $\gamma = \sqrt{2}$; however, $\gamma \approx 1.2$ yields atomic mean excitation energies from the local plasma model in better agreement with the accurate atomic values calculated by Dehmer et al. (ref. 6). The fact that the larger value ($\gamma = \sqrt{2}$) gives better agreement with empirical data suggests that this larger value corrects (in addition to individual electron shifts) for the chemical shifts as well. Such chemical shifts were estimated separately for covalent and ionic bonds in references 35 and 36.

Encouraged by the smallness (<30 percent) of the empirical individual electron corrections to the collective plasma frequency (refs. 32, 35, and 36), a calculation (ref. 37) in which individual electron shifts were estimated according to the theory for plane-wave states in an extended plasma, as calculated by Pines (ref. 22), yields results that are in good agreement with Dehmer et al. (ref. 6). Consequently, the local plasma model is placed on a parameter-free basis in which chemical shifts are determined from atomic molecular parameters alone, and effects of individual electron motion are evaluated in terms of the Pines correction, the combined effects of which are on the order of the plasma frequency shift of $\gamma \approx \sqrt{2}$ suggested by Lindhard and Scharff.

The Pines correction makes a remarkable improvement in the prediction of the local plasma model, and further adjustments in the theory, to account for the plasma frequency shifts resulting from the atomic shell structure, should bring the model into accurate predictive capability. To further elucidate the relationship between the local plasma model and the more exact quantum treatment of bonded systems, related quantities of both theories in the case of one- and two-electron systems are examined in the following section of this report. Atomic mean excitation energies and straggling parameters, based on the local plasma model, are compared with accurate calculations of Inokuti et al. (refs. 6 to 8) in the section entitled "Stopping and Straggling Parameters of Atoms." The use of the Gordon-Kim electron gas model of molecular bonding (ref. 38) to determine the effects of covalent chemical bond shifts on mean excitation energy for elements of the first two rows is presented in the section entitled "Covalent-Bond Effects." Calculations of mean excitation energies of ionic-bonded substances are discussed in the section entitled "Ionic-Bond

Effects," and the mean excitation energies of metals are discussed in the section entitled "Metallic-Bond Effects."

EXCITATION SPECTRA OF ONE- AND TWO-ELECTRON SYSTEMS

The hydrogen atomic excitation spectrum in the dipole approximation is well known as

$$f_H(\omega) = \begin{cases} \displaystyle\sum_{n=2} \frac{2^8}{3}\left(1 - \frac{1}{n^2}\right) n^7 \frac{(n-1)^{2n-5}}{(n+1)^{2n+5}}\, \delta(\omega - \omega_n) & (\hbar\omega < R) \\ \displaystyle\frac{1}{2}\sqrt{\frac{\hbar}{RW}}\, \frac{2^8}{3}\, \hbar\omega\, \frac{k}{(1+k^2)^5}\, \frac{\exp\left(-\frac{4}{k}\arctan k\right)}{1 - \exp(-2\pi/k)} & (\hbar\omega > R) \end{cases} \tag{25}$$

where n is the principal quantum number, R is Rydberg's constant, ω_n is given by

$$\hbar\omega_n = R(1 - 1/n^2) \tag{26}$$

and

$$Rk^2 = \hbar\omega - R \tag{27}$$

The corresponding spectrum for the local plasma model (eq. (20)) is given as

$$f_p(\omega) = \begin{cases} 4\omega\omega_o^{-2} \ln^2(\omega/\omega_o) & (\omega < \omega_o) \\ 0 & (\omega > \omega_o) \end{cases} \tag{28}$$

Where $\hbar\omega_o = 55.12$ eV. The cumulative oscillator strength

$$F(\omega) = \int_0^{\omega} f(\omega')\, d\omega' \tag{29}$$

is shown in figure 1 for each of the two models. Similarly, the excitation spectrum of the helium atom has been evaluated for screened wave functions and is shown in figure 1. The fractional excitations of the two models never differ by more than ≈15 percent above the excitation threshold. As noted by Dehmer et al. (ref. 6), the main error in the local plasma model is the contribution to absorption below excitation threshold all the way down to zero. This error is also evident in the energy

moments of the plasma model. The moments of the energy spectrum for the hydrogen atom are shown in figure 2, where

$$\langle (E/R)^m \rangle = \int_0^\infty \left(\frac{\hbar\omega}{R}\right)^m f(\omega)\, d\omega \tag{30}$$

and m is a continuous parameter. The low-frequency contributions associated with the local plasma model cause a divergence in equation (30) at $m \approx -2$ which is not present in the quantum system. Atomic polarizability and the low-frequency refractive index are affected the most. Other atomic properties, such as the total inelastic cross section, the mean excitation energy, the straggling parameter, and the mean electronic kinetic energy, are reasonably represented by the plasma model. Also shown in figure 2 are results, including the Pines correction (ref. 22) to the plasma frequency, which indicate substantial improvement in the prediction of atomic properties, although low-energy atomic properties are still beyond the scope of the model.

The plasma model is expected to be more accurate as more electrons are added to the system. This occurs in two ways, as seen in figure 1. First, a greater contribution comes from the continuum, which is most like the plasma. Second, the excitation thresholds shift to relatively lower energies and fill in the low-frequency region, for which the plasma model normally tends to error. A considerable improvement in the energy moments of helium for the local plasma approximation are clearly shown in figure 3.

The moments of the excitation spectrum of H_2 have been evaluated empirically by using experimental oscillator strengths (ref. 39) and theoretically (ref. 14) using the Dalgarno sum rules of reference 12 (eqs. (4) to (6)). These are compared in figure 4 with an "atomic" approximation to H_2 taken as a generalization of Bragg's rule (ref. 11). Also shown in figure 4 are values for H_2 calculated using the local plasma model with the Pines correction and with the Gordon-Kim model of the molecular wave functions (ref. 38) given as

$$\rho_{H_2}(\vec{r}) = \rho_H(\vec{r}) + \rho_H(\vec{r} - \vec{R}) \tag{31}$$

where $\rho_H(\vec{r})$ is the atomic hydrogen electron density and $\vec{R}$ is the displacement vector of length $1.4a_o$ between the two centers. It is clear from figure 4 that, even with the simple Gordon-Kim approximation, the plasma model is a considerable improvement over the Bragg rule, except for the lowest-energy molecular properties (i.e., $m < -0.5$). Figure 4 also shows that the Gordon-Kim approximation introduces minor errors compared with the inherent limitations of the local plasma model.

The mean excitation energy for stopping power may likewise be evaluated. Atomic and molecular hydrogen are compared in table I with a recent compilation of experimental data (ref. 40). Quite reasonable estimates of atomic and molecular properties of importance to ionizing radiation are obtained by this local plasma model if the Pines correction is included. Optical and other low-frequency properties, however, are poorly represented. The plasma model should become more accurate for more complex many-electron systems, especially those in which the optical properties are more in line with those predicted by the plasma model.

With the present results, it is now clear what approach should be taken to improve the plasma model applications. Clearly, a correction factor similar to that

of Pines should be introduced to suppress absorption below excitation threshold and, correspondingly, to enhance frequencies just above threshold. A number of possibilities are open to implement such a correction, which would appear as a first-order quantum correction for the discrete spectrum. Preliminary work by Walecka (ref. 41) on the study of collective atomic oscillations may be a starting point for further development.

STOPPING AND STRAGGLING PARAMETERS OF ATOMS

In this section, parameters are considered for atoms associated with the stopping of charged particles and fluctuations in their energy transfer. The energy moment is

$$S(m) = \langle (E/R)^m \rangle \tag{32}$$

and the related quantity is

$$L(m) = \frac{dS(m)}{dm} \tag{33}$$

In terms of these quantities, the mean excitation energy is

$$\ln I = L(0)/S(0) \tag{34}$$

and the straggling parameter related to fluctuations in energy loss is

$$\ln \Delta = L(1)/S(1) \tag{35}$$

The mean excitation energy (eq. (34)) has been evaluated in the context of the local plasma model and is compared in figure 5 with the values computed by Inokuti and co-workers (refs. 6 to 8) for atoms through krypton. Hartree-Fock wave functions (ref. 42) have been used through neon and sodium through krypton are represented by screened wave functions (ref. 43).

The values for the straggling parameter were similarly evaluated and are compared in figure 6 with the values obtained by Inokuti and co-workers. Also shown are values for noble gases compiled by Inokuti et al. (refs. 6 to 8) and values obtained by Zeiss et al. (ref. 11). The present values tend to be about 25 percent low at $Z \approx 36$, with improvements at lower values of Z, which may be caused by the lack of shell structure corrections in the plasma frequencies of the K and L shells.

It is clear from these atomic calculations that the plasma model with the Pines correction generally provides good results for mean excitation energy and reasonable estimates for the straggling parameter. Although Hartree-Fock wave functions are required for low atomic numbers, reasonable results are obtained using screened wave functions for atoms heavier than argon. It is mainly the low-energy atomic

properties which require improvements beyond the Pines correction. These properties emphasize the need for a first-order quantum correction to the atomic structure.

COVALENT-BOND EFFECTS

Early experimental work with ionization energy loss was conducted in covalent-bonded gases (also noble gases), from which Bragg's rule was derived. Although more recent experimental work, beginning with Thompson (ref. 44), has shown systematic variation from Bragg's rule, such rules still seem appropriate for fixed molecular structures (refs. 45 and 46). As the result of the theoretical efforts of Inokuti and co-workers (refs. 6 to 8), it is clear that chemical-bond shifts in the mean excitation energy have occurred, and, as suggested by Platzman (ref. 5), all covalent shifts are of similar magnitude.

In any molecular dynamic calculation, there is a trade-off between model accuracy and computational efficiency. As pertains to the radiolysis of large molecular structures, the most useful model is the lowest order possible. It is clear that the use of self-consistent field methods to determine molecular wave functions would seriously limit the ability to study systems of practical interest. Considering the relative success of the Gordon-Kim electron gas model of molecular bonding (refs. 38, 47, and 48), a simple method for the calculation of chemical-bond effects on the mean excitation energies is suggested. As suggested by Gordon and Kim, the molecular electron density as a superposition of the unperturbed atomic states is given by

$$\rho(\vec{r}) = \rho_1(\vec{r}) + \rho_2(\vec{r} - \vec{R}_{12}) \tag{36}$$

for diatomic molecules. There is an obvious generalization of equation (36) for the polyatomic case. Whereas Gordon and Kim used equation (36) to calculate the molecular potential (see refs. 47 and 48 for ionic and covalent applications) from which R_{12} is theoretically obtained, R_{12} is taken here from observed experimental bond distances. Substituting equation (36) into equations (14) and (18) and reducing results in

$$Z \ln(I) = Z_1 \ln(I_1) + \int \rho_1(\vec{r}) \ln[1 + \rho_2(\vec{r} - \vec{R}_{12})/\rho_1(\vec{r})]^{1/2} \, d^3r$$

$$+ Z_2 \ln(I_2) + \int \rho_2(\vec{r}) \ln[1 + \rho_1(\vec{r} - \vec{R}_{21})/\rho_2(\vec{r})]^{1/2} \, d^3r \tag{37}$$

where I_1 and I_2 are the corresponding atomic values, which are accurately known (refs. 6 to 8). The chemical bonding correction is generally

$$\ln(1 + \delta_{ij}) = \frac{1}{Z_i} \int \rho_i(\vec{r}) \ln[1 + \rho_i(\vec{r} - \vec{R}_{ij})/\rho_i(\vec{r})]^{1/2} \, d^3r \tag{38}$$

Generalizing equation (37) yields

$$Z \ln(I) = \sum_i Z_i \ln\left[\left(1 + \sum_j \delta_{ij}\right) I_i\right] \tag{39}$$

where the sum over j includes every bond in which Z is attached in the molecule. Correction factors have been calculated (ref. 35) for hydrogen and carbon molecules with the bond parameters in table II. Carbon sp^3 hybrid orbital wave functions were used in these calculations, although s^2p^2 values were only slightly different. The tetrahedral orbitals were spherically symmetrical in their electron densities. Therefore, spherical symmetry was assumed throughout subsequent calculations.

Recommended values of mean excitation energies (ref. 40) are compared in table III with theoretical values calculated using atomic mean excitation energies from Dehmer et al. (ref. 6) with the bond corrections in table II. Bragg's rule is also used with the atomic values of Dehmer et al. for comparison. Although the theoretical values are within 4 percent of the experimental and empirical values, the Bragg's rule values are from 17 to 21 percent low, indicating a substantial adjustment as the result of chemical bonding.

Mean excitation energies have been calculated for covalent gases of the first two rows using the local plasma model and the Pines correction. Results are compared with empirical values (ref. 40) in table IV. Corresponding values for covalent solids are shown in table V.

Moments for the N_2 molecule using the plasma model are compared in figure 7 with values calculated from the oscillator strengths compiled by Dalgarno et al. (ref. 49). As can be seen, good agreement between the present simple plasma model calculations and the oscillator strength distribution of reference 49 is obtained except for the lowest-frequency phenomena.

IONIC-BOND EFFECTS

Although covalent bond shifts were found to be relatively small corrections to atomic values, such a separation as in equation (37) in terms of neutral atomic values are not possible for ionic bonds. Using the Gordon-Kim model electron density of the partial ionic (diatomic) system,

$$\rho_p(\vec{r}) = \rho_{A^{(+p)}}(\vec{r}) + \rho_{B^{(-p)}}(\vec{r} - \vec{R}_{AB}) \tag{40}$$

where $A^{(+p)}$ and $B^{(-p)}$ refer to partially ionic states of the two constituents, $\vec{R}_{AB}$ is their nuclear separation, and p is the partial ionic fraction. The electron density of a partial ionic atom in equation (40) is

$$\rho_{A^{(\pm p)}}(\vec{r}) = (1 - p)\,\rho_A(\vec{r}) + p\,\rho_{A^{\pm}}(\vec{r}) \tag{41}$$

where $\rho_A(\vec{r})$ is the electron density of the neutral atom and $\rho_{A^{\pm}}(\vec{r})$ is the electron density of the atomic ion. With the aid of equations (40) and (41), shifts in

the mean excitation energy caused by ionic and covalent effects can be evaluated. As shown in reference 36,

$$Z \ln(I) = Z_{A(+p)} \ln\left[I_{A(+p)}\right] + \int \rho_{A(+p)}(\vec{r}) \ln\left[1 + \rho_{B(-p)}(\vec{r} - \vec{R}_{AB}) \Big/ \rho_{A(+p)}(\vec{r})\right]^{1/2} d^3r$$

$$+ Z_{B(-p)} \ln\left[I_{B(-p)}\right] + \int \rho_{B(-p)}(\vec{r}) \ln\left[1 + \rho_{A(+p)}(\vec{r} - \vec{R}_{AB}) \Big/ \rho_{B(-p)}(\vec{r})\right]^{1/2} d^3r \qquad (42)$$

with

$$Z_{A(+p)} \ln\left[I_{A(+p)}\right] = \int \rho_{A(+p)}(\vec{r}) \ln\left[\gamma\hbar\omega_{A(+p)}(\vec{r})\right] d^3r \qquad (43)$$

where γ is the Pines correction given by equation (15) or estimated empirically as in reference 46. Mean excitation energies for various stages of ionization calculated using the Pines correction and the atomic wave functions of Clementi and Roetti (ref. 42) are shown in figure 8. In addition to the the ionic-bond shifts, there are shifts caused by covalent-like character, as given by

$$\ln\left[1 + \delta_{A(+p),B(-p)}\right] = \frac{1}{Z_{A(+p)}} \int \rho_{A(+p)}(\vec{r}) \ln\left[1 + \rho_{B(-p)}(\vec{r} - \vec{R}) \Big/ \rho_{A(+p)}(\vec{r})\right]^{1/2} d^3r \qquad (44)$$

Mean excitation energies for partial ionic-bonded substances are shown in table VI with the corresponding bond parameters used in the model. Also shown are values for a pure covalent bond and Bragg values using the neutral atomic mean excitation energies of Dehmer et al. (ref. 6) as well as Bragg values of the corresponding partial ionic states. The ionic-bond fractions are taken from Pauling (ref. 50) as experimental data for HF and LiH. Bond lengths are for ionic crystals except for the HF gas. Atomic mean excitation energies are shown for partial ionic states in figure 8, and differ from values in reference 36 because of the Pines correction.

It is clear from table VI that the main contribution to corrections to the Bragg rule is the adjustment from atomic neutral to atomic ion mean excitation energies as proposed by Platzman (ref. 5). Indeed, when there is little difference between the usual Bragg value and the partially ionic Bragg value, the covalent value is in near agreement with the predicted value of I for HF and LiH in the table. For LiF, the relatively large adjustment from the usual Bragg value (81.6) to the partially ionic Bragg value (92.6) leaves a large difference between the covalent value (83.4) and the predicted value of I (93.6). The adjustment of the ionic-bond shift caused by the covalent-like character for LiF is 1 eV compared with adjustments of the neutral states caused by the pure covalent bond of 1.8 eV. This comparison shows the greater role of the Coulomb attraction in forming the bond of the ionic molecules relative to the two-electron interaction in forming the covalent bond.

Calculated mean excitation energies for ionic crystals using the Pines correction are shown in table VII, along with recommended values (ref. 40). The crystal parameter and fractional ionic charge have been taken from Pauling (ref. 50). The LiF value is the only one with an experimental basis (ref. 36).

METALLIC-BOND EFFECTS

The first approach to metals in this paper is similar to that taken by Chu et al. (ref. 30), in which they employed the muffin-tin wave functions (ref. 31) and stopping-power theory according to Lindhard and Winther (ref. 24). Individual electron corrections to the local plasma frequency are treated empirically through an adjustable parameter γ. (See table I of (ref. 32) and related discussion.) Unlike this previous work, the present work includes estimates of shifts in the plasma frequency according to the Pines correction in equation (15) and is in that sense completely deterministic.

The metallic wave functions for lithium metal approximated by the Wigner-Seitz model (ref. 51) are considered first. In deriving these wave functions, the lithium ion core potential was taken from the screened wave functions of Clementi and Raimondi (ref. 43), and the calculated crystal-valence wave functions (aside from normalization) were found to be a slight perturbation (mainly due to boundary conditions) of the free hydrogenic (2s) orbital inside the Wigner-Seitz sphere. The final crystal wave functions used were constructed from unperturbed Hartree-Fock orbitals (ref. 42) in the core region with a small perturbation outside the core. This perturbation matched the boundary conditions on the surface of the Wigner-Seitz sphere (ref. 51). This was followed by normalization of the valence-shell wave functions (to make the valence electron density add up to give the correct number of valence electrons). These wave functions are quite similar to the muffin-tin model (ref. 31) and yield mean excitation energies in substantial agreement with Ziegler (ref. 32) when γ is taken as his empirical value. The mean excitation energies for metals of the second and third row using Wigner-Seitz wave functions (treating all valence electrons as spatially equivalent) and the Pines correction are compared in table VIII with empirical values (ref. 40).

The present results clearly demonstrate that the effects of the metallic bond in lithium and beryllium are large and are mainly the result of collective oscillations in the free-electron gas formed by the valence electrons. Although similar good agreement should be expected for sodium and magnesium, it is emphasized here only that these empirical values are interpolations without an experimental basis, and smaller empirical values more in line with the present results should not be eliminated. The small value predicted for aluminum (149 eV) is in doubt, as the empirical value (166 ± 4 eV) is based on one of the most experimentally studied quantities since aluminum served as a standard in stopping-power experiments for many years. The fault could well lie in the use of the Wigner-Seitz model for group III metals. It is well-known that the success of the Wigner-Seitz theory rests mainly on application to alkali metals. Although some hope for application to group II metals exists, treating the three valence electrons of group III as spatially equivalent is clearly in error. Correction to metals from an alternate model, proposed by Pauling (ref. 50) for metallic orbitals and implemented here in simplified fashion, are considered next.

In X-ray diffraction experiments, even beryllium metal shows a considerable degree of covalent quality, as suspected from bulk material properties (ref. 52). In this view, a model is considered in which the valence-bond effects can be included explicitly. In the spirit of the Pauling valence-bond theory (ref. 50) and the Gordon-Kim model (ref. 38) of valence bonding, the electron density about the ion cores is assumed to be a superposition of partial ionic core states among nearest core neighbors. Additional contributions from next-nearest neighbors are assumed to add to the electron continuum states in a manner analogous to the Pauling

unsynchronized resonances in lithium crystals (ref. 50). The electron density of the partially ionic core charge p is

$$\rho_{A(+p)}(\vec{r}) = \left(\frac{v - p}{v}\right)\rho_A(\vec{r}) + \frac{p}{v}\rho_{A(+v)}(\vec{r}) \tag{45}$$

where v is the number of valence electrons, $\rho_A(\vec{r})$ is the electron density of the atomic neutral state, and $\rho_{A(+v)}(\vec{r})$ is the electron density of the valence-stripped ion cores. We have used the observation by Slater that radial wave functions of the L shell are nearly the same for both values of ℓ as a result of exchange interaction between the (2s) and (1s) orbitals. The same is true for the M shell. In the present calculation, each metal ion core has been placed into a Wigner-Seitz cell and the electron density from nearest neighbors has been approximated by reflecting the exterior core density function across the cell boundary. The continuum electron density is then taken as

$$\rho_e = [p + (v - p)\delta](3/4\pi r_s^3) \tag{46}$$

where δ is the next-nearest-neighbor contribution to the continuum. The value of δ is determined by requiring a full complement of v valence electrons per cell. The resultant electron density $\rho(r)$ was used to calculate the local plasma frequency and mean excitation energy per cell. The Pines correction was used for individual particle shifts. The radii r_s for the Wigner-Seitz cell are given in table VIII. The ion-core wave functions were calculated from the Hartree-Fock wave functions of Clementi and Roetti (ref. 42). A slight dependence on the ion-core charge appears (ref. 53) in which there is some increase in mean excitation to $I = 155$ eV for aluminum. However, there are some unresolved questions, concerning periodicity at the cell boundaries, which leave the value of this model in doubt.

The mean excitation energy for aluminum requires the reconsideration of the data on which it is based and the corresponding analysis. In an analysis by Andersen and Ziegler (ref. 54), 162 eV was assumed as the mean excitation energy for aluminum. A reduction in I to 150 eV results in a 3-percent increase in stopping power at 1 MeV, which leaves it within the stated uncertainty limits of the Andersen and Ziegler parametric curves (ref. 54). These curves correspond to the uncertainty in the experimental data used in the analysis of reference 54. (See fig. 9.) Indeed, a number of authors have reported mean excitation energies for aluminum in line with the present results (refs. 55 to 60), although more recent analyses are higher. A recent study of aluminum optical properties indicates that a value of I several eV lower than 166 eV is not inconsistent with the empirical dielectric function (ref. 61). The shift of several eV is associated with polarization of the $A\ell^{3+}$ core by the valence electrons in their metallic orbitals. Such core polarization effects are not calculated in the present model. Furthermore, quantum corrections to K- and L-shell discrete spectrum may cause further small adjustments. In any case, the apparent discrepancy is due to the electronic wave functions used in the present calculation, to the inadequate treatment of corrections to the Bethe formula, from which I is extracted from the experimental data (see for example refs. 62 and 63), to quantum corrections, or to a combination of these.

To further clarify the relationship between the mean excitation energy for aluminum and experimental data, a band is shown in figure 9 which brackets the experi-

mental data in references 62 and 64 to 68 for proton energies between 0.5 and 10 MeV. These energies are compared with the reduced stopping power calculated from the Andersen and Ziegler empirical shell corrections (ref. 54). The older data of Kahn (ref. 64), which would have lowered the band considerably, were excluded from the figure. The mean excitation energies exhibited in the figure are the 167 eV used as input to Shiles et al. (ref. 61), the 162 eV determined by Andersen and Ziegler (ref. 54), the 155 eV estimated using one form of valence-bond theory, and the 149 eV calculated according to the present (simplified) Wigner-Seitz model. While it is not clear that the 167-eV curve is superior to the 149-eV curve, a modest shift in the empirical shell corrections can bring any of the four curves into an equally good fit to the data. It is further emphasized that shell corrections are not exactly known nor in empirical analysis are shell corrections usually differentiated from other corrections to the Bethe formula (eq. (1)).

DISCUSSION

The present results are combined in figure 10 with the evaluated data of Seltzer and Berger (ref. 40). Care is taken where possible to model the same physical-chemical state. (See specific tables for details.) Results for free atoms (Hartree-Fock wave functions for $Z \leq 10$, and screened wave functions elsewhere) are also compared in figure 10 with the accurate atomic values of Dehmer et al. (ref. 6). It is clear that the trends in the first- and second-period elements are well approximated by the present application of the local plasma model, especially when the Pines correction is applied. The present results are generally in fair agreement with the compilation and recommendations of Seltzer and Berger (ref. 40), although small discrepancies in the third period remain to be resolved.

Perhaps the greatest criticism of the present application of the local plasma model calculations is the use of the Gordon-Kim approximation to the covalent-bonded wave functions. When the moments of the energy spectrum are considered, it is clear that the Gordon-Kim model approximately adjusts the excitation spectrum in the region of greatest importance to ionizing radiation, and appears no more in error than the basic plasma model in which it is used. (See fig. 4.) Of course, accurate use of the plasma model implies the necessary use of the Pines correction, as demonstrated for the hydrogen atom in figure 2 and used throughout the present calculations. Although the Pines correction produces marked improvements in the predictive capability of the model, further quantum corrections for the discrete spectrum would produce additional corrections and would hopefully remove most of the remaining error in the plasma model. Further improvement in electronic wave functions would be helpful in identifying the remaining corrections required for the plasma model.

ACKNOWLEDGMENTS

The authors wish to express their gratitude to Govind S. Khandelwal of Old Dominion University, Willard E. Meador of the Langley Research Center, Mito Inokuti

of the Argonne National Laboratory, and Stephen Seltzer of the National Bureau of Standards for helpful discussions and encouragement. Special thanks are offered to Stephen Seltzer, Martin Berger, and Mito Inokuti for sharing unpublished data.

Langley Research Center
National Aeronautics and Space Administration
Hampton, VA 23665
February 3, 1984

REFERENCES

1. Bohr, N.: On the Decrease of Velocity of Swiftly Moving Electrified Particles in Passing Through Matter. Philos. Mag. & J. Sci., ser. 6, vol. 30, no. 175, July 1915, pp. 581-612.

2. Bethe, Von H.: Zur Theorie des Durchgangs schneller Korpuskularstrahlen durch Materie. Ann. Phys., 5 Folge, Bd. 5, 1930, pp. 325-400.

3. Walske, M. C.; and Bethe, H. A.: Asymptotic Formula for Stopping Power of K-Electrons. Phys. Rev., vol. 83, 1951, pp. 457-458.

4. Bragg, W. H.; and Kleeman, R.: On the α Particles of Radium, and Their Loss of Range in Passing Through Various Atoms and Molecules. Philos. Mag. & J. Sci., ser. 6, vol. 10, no. 57, Sept. 1905, pp. 318-340.

5. Platzman, Robert L.: Influences of Details of Electronic Binding on Penetration Phenomena, and the Penetration of Energetic Charged Particles Through Liquid Water. Symposium on Radiobiology - The Basic Aspects of Radiation Effects on Living Systems, James J. Nickson, ed., John Wiley & Sons, Inc., c.1952, pp. 139-176.

6. Dehmer, J. L.; Inokuti, Mitio; and Saxon, R. P.: Systematics of Moments of Dipole Oscillator-Strength Distributions for Atoms of the First and Second Row. Phys. Rev. A, third ser., vol. 12, no. 1, July 1975, pp. 102-121.

7. Inokuti, Mitio; Baer, T.; and Dehmer, J. L.: Addendum: Systematics of Moments of Dipole Oscillator-Strength Distributions for Atoms in the First and Second Row. Phys. Rev. A, vol. 17, no. 3, Mar. 1978, pp. 1229-1231.

8. Inokuti, M.; Dehmer, J. L.; Baer, T.; and Hanson, J. D.: Oscillator-Strength Moments, Stopping Powers, and Total Inelastic-Scattering Cross Sections of All Atoms Through Strontium. Phys. Rev. A, vol. 23, no. 1, Jan. 1981, pp. 95-109.

9. Dalgarno, A.: The Stopping Powers of Atoms. Proc. Phys. Soc. (London), vol. 76, pt. 3, no. 489, Sept. 1, 1960, pp. 422-424.

10. Zeiss, G. D.; and Meath, W. J.: The H_2O-H_2O Dispersion Energy Constant and the Dispersion of the Specific Refractivity of Dilute Water Vapour. Mol. Phys., vol. 30, no. 1, July 1975, pp. 161-169.

11. Zeiss, G. D.; Meath, William J.; MacDonald, J. C. F.; and Dawson, D. J.: Accurate Evaluation of Stopping and Straggling Mean Excitation Energies for N, O, H_2, N_2, O_2, NO, NH_3, H_2O, and N_2O Using Dipole Oscillator Strength Distributions - A Test of the Validity of Bragg's Rule. Radiat. Res., vol. 70, no. 2, May 1977, pp. 284-303.

12. Dalgarno, A.: Sum Rules and Atomic Structure. Rev. Mod. Phys., vol. 35, no. 3, July 1963, pp. 522-524.

13. Chan, Y. M.; and Dalgarno, A.: The Stopping Powers of Atoms and Molecules. Proc. Phys. Soc. (London), vol. 85, 1965, pp. 457-459.

14. Kamikawai, Ryotaro; Watanabe, Tsutomu; and Amemiya, Ayao: Mean Excitation Energy for Stopping Power of Molecular Hydrogen. Phys. Rev., second ser., vol. 184, no. 2, Aug. 10, 1969, pp. 303-311.

15. Landau, L. D.; and Lifshitz, E. M.: Electrodynamics of Continuous Media. Addison-Wesley Pub. Co., Inc., 1960.

16. Ahlen, Steven P.: Theoretical and Experimental Aspects of the Energy Loss of Relativistic Heavily Ionizing Particles. Rev. Mod. Phys., vol. 52, no. 1, Jan. 1980, pp. 121-173.

17. Kramers, H. A.: The Stopping Power of a Metal for α-Particles. Physica, vol. 13, 1947, pp. 401-412.

18. Lindhard, J.: On the Properties of a Gas of Charged Particles. Mat.-Fys. Medd. - K. Dan Vidensk. Selsk., vol. 28, no. 8, 1954.

19. Bohm, David; and Pines, David: A Collective Description of Electron Interactions. I. Magnetic Interactions. Phys. Rev., second ser., vol. 82, no. 5, June 1, 1951, pp. 625-634.

20. Pines, David; and Bohm, David: A Collective Description of Electron Interactions. II. Collective vs Individual Particle Aspects of the Interactions. Phys. Rev., second ser., vol. 85, no. 2, Jan. 15, 1952, pp. 338-353.

21. Bohm, David; and Pines, David: A Collective Description of Electron Interactions. III. Coulomb Interactions in a Degenerate Electron Gas. Phys. Rev., second ser., vol. 92, no. 3, Nov. 1, 1953, pp. 609-625.

22. Pines, David: A Collective Description of Electron Interactions: IV. Electron Interaction in Metals. Phys. Rev., second ser., vol. 92, no. 3, Nov. 1, 1953, pp. 626-636.

23. Lindhard, Jens; and Scharff, Morten: Recent Developments in the Theory of Stopping Power. 1. Principles of the Statistical Method. Penetration of Charged Particles in Matter, Edwin Albrecht Uehling, ed., Nucl. Sci. Ser. Rep. No. 29 (Publ. 752), Natl. Acad. Sci.-Natl. Res. Counc., 1960, pp. 49-55.

24. Lindhard, J.; and Winther, A.: Stopping Power of Electron Gas and Equipartition Rule. Mat.-Fys. Medd. - K. Dan. Vidensk. Selsk., vol. 34, no. 4, 1964.

25. Walske, M. C.: The Stopping Power of K-Electrons. Phys. Rev., second ser., vol. 88, no. 6, Dec. 15, 1952, pp. 1283-1289.

26. Chu, W. K.; and Powers, D.: Calculations of Mean Excitation Energy for All Elements. Phys. Lett., vol. 40A, no. 1, June 19, 1972, pp. 23-24.

27. Rousseau, C. C.; Chu, W. K.; and Powers, D.: Calculations of Stopping Cross Sections for 0.8- to 2.0-MeV Alpha Particles. Phys. Rev. A, third ser., vol. 4, no. 3, Sept. 1971, pp. 1066-1070.

28. Bonderup, E.: Stopping of Swift Protons Evaluated From Statistical Atomic Model. Mat.-Fys. Medd. - K. Dan. Vidensk. Selsk., vol. 35, no. 17, 1967.

29. Chu, W. K.; and Powers, D.: Alpha-Particle Stopping Cross Section in Solids From 400 KeV to 2 MeV. Phys. Rev., second ser., vol. 187, no. 2, Nov. 10, 1969, pp. 478-490.

30. Chu, W. K.; Moruzzi, V. L.; and Ziegler, J. F.: Calculations of the Energy Loss of ^{4}He Ions in Solid Elements. J. Appl. Phys., vol. 46, no. 7, July 1975, pp. 2817-2820.

31. Moruzzi, V. L.; Janak, J. F.; and Williams, A. R.: Calculated Electronic Properties of Metals. Pergamon Press, Inc., c.1978.

32. Ziegler, J. F.: The Stopping of Energetic Ions in Solids. Nucl. Instrum. & Methods, vol. 168, nos. 1-3, Jan. 1-15, 1980, pp. 17-24.

33. Hubbard, J.: The Dielectric Theory of Electronic Interactions in Solids. Proc. Phys. Soc. (London), vol. 68, pt. 11, no. 431A, Nov. 1, 1955, pp. 976-986.

34. Fröhlich, H.; and Pelzer, H.: Plasma Oscillations and Energy Loss of Charged Particles in Solids. Proc. Phys. Soc. (London), vol. 68, pt. 6, no. 426A, June 1, 1955, pp. 525-529.

35. Wilson, J. W.; and Kamaratos, E.: Mean Excitation Energy for Molecules of Hydrogen and Carbon. Phys. Lett., vol. 85A, no. 1, Sept. 7, 1981, pp. 27-29.

36. Wilson, J. W.; Chang, C. K.; Xu, Y. J.; and Kamaratos, E.: Ionic Bond Effects on the Mean Excitation Energy for Stopping Power. J. Appl. Phys., vol. 53, no. 2, Feb. 1982, pp. 828-830.

37. Wilson, J. W.; and Xu, Y. J.: Metallic Bond Effects on Mean Excitation Energies for Stopping Power. Phys. Lett., vol. 90A, no. 5, July 12, 1982, pp. 253-255.

38. Gordon, Roy G.; and Kim, Yung Sik: Theory for the Forces Between Closed-Shell Atoms and Molecules. J. Chem. Phys., vol. 56, no. 6, Mar. 15, 1972, pp. 3122-3133.

39. Dalgarno, A.; and Williams, D. A.: Properties of the Hydrogen Molecule. Proc. Phys. Soc. (London), vol. 85, pt. 4, no. 546, Apr. 1965, pp. 685-689.

40. Seltzer, S. M.; and Berger, M. J.: Evaluation of the Collision Stopping Power of Elements and Compounds for Electrons and Positrons. Int. J. Appl. Radiat. & Isot., vol. 33, no. 11, Nov. 1982, pp. 1189-1218.

41. Walecka, J. D.: Collective Excitations in Atoms. Phys. Lett., vol. 58A, no. 2, Aug. 9, 1976, pp. 83-86.

42. Clementi, Enrico; and Roetti, Carla: Roothaan-Hartree-Fock Atomic Wavefunctions. At. Data & Nucl. Data Tables, vol. 14, nos. 3-4, Sept.-Oct. 1974, pp. 177-478.

43. Clementi, E.; and Raimondi, D. L.: Atomic Screening Constants From SCF Functions. J. Chem. Phys., vol. 38, no. 11, June 1, 1963, pp. 2686-2689.

44. Thompson, Theos Jardin: Effect of Chemical Structure on Stopping Powers for High-Energy Protons. UCRL-1910, Univ. of California, Aug. 11, 1952.

45. Lodhi, A. S.; and Powers, D.: Energy Loss of α Particles in Gaseous C-H and C-H-F Compounds. Phys. Rev. A, vol. 10, no. 6, Dec. 1974, pp. 2131-2140.

46. Neuwirth, Wolfgang; Pietsch, Werner; and Kreutz, Ronald: Chemical Influences on the Stopping Power. Nucl. Instrum. & Methods, vol. 149, nos. 1-3, Feb. 15-Mar. 1, 1978, pp. 105-113.

47. Tossell, J. A.: Calculation of Bond Distances and Cohesive Energies for Gaseous Halides Using the Modified Electron Gas Ionic Model. Chem. Phys. Lett., vol. 67, no. 2-3, Nov. 15, 1979, pp. 359-364.

48. Waldman, Marvin; and Gordon, Roy G.: Scaled Electron Gas Approximation for Intermolecular Forces. J. Chem. Phys., vol. 71, no. 3, Aug. 1, 1979, pp. 1325-1339.

49. Dalgarno, A.; Degges, T.; and Williams, D. A.: Dipole Properties of Molecular Nitrogen. Proc. Phys. Soc. (London), vol. 92, pt. 2, no. 576, Oct. 1967, pp. 291-295.

50. Pauling, Linus: The Chemical Bond. Cornell Univ. Press, c.1967.

51. Wigner, E. P.; and Seitz, F.: On the Constitution of Metallic Sodium. II. Phys. Rev., second ser., vol. 46, no. 6, Sept. 15, 1934, pp. 509-524.

52. Brown, P. J.: A Study of Charge Density in Beryllium. Philos. Mag., vol. 26, no. 6, Dec. 1972, pp. 1377-1394.

53. Kamaratos, E.; Chang, C. K.; Wilson, J. W.; and Xu, Y. J.: Valence Bond Effects on Mean Excitation Energies for Stopping Power in Metals. Phys. Lett., vol. 92A, no. 7, Nov. 29, 1982, pp. 363-365.

54. Andersen, H. H.; and Ziegler, J. F.: Hydrogen Stopping Powers and Ranges in All Elements. Pergamon Press, Inc., c.1977.

55. Bakker, C. J.; and Segrè, E.: Stopping Power and Energy Loss for Ion Pair Production for 340-Mev Protons. Phys. Rev., second ser., vol. 81, no. 4, Feb. 15, 1951, pp. 489-492.

56. Simmons, D. H.: The Range-Energy Relation for Protons in Aluminum. Proc. Phys. Soc. (London), vol. 65, pt. A, 1952, pp. 454-456.

57. Mather, R.; and Segrè, E.: Range Energy Relation for 340-Mev Protons. Phys. Rev., second ser., vol. 84, no. 2, Oct. 15, 1951, pp. 191-193.

58. Sachs, Donald C.; and Richardson, J. Reginald: Mean Excitation Potentials. Phys. Rev., second ser., vol. 89, no. 6, Mar. 15, 1953, pp. 1163-1164.

59. Bogaardt, M.; and Koudijs, B.: On the Average Excitation Potentials and the Range-Energy Relations in Light Elements. Physica, vol. 18, Apr. 1952, pp. 249-264.

60. Vasilevskii, I. M.; and Prokoshkin, Yu. D.: Ionizatsionnye Potentsialy Atomov (Ionization Potentials of Atoms). Dubna:Ob'edinen. Inst. Yadernykh Issledovanni, 1960.

61. Shiles, E.; Sasaki, Taizo; Inokuti, Mitio; and Smith, D. Y.: Self-Consistency and Sum-Rule Tests in the Kramers-Kronig Analysis of Optical Data: Applications to Aluminum. Phys. Rev. B, vol. 22, no. 4, Aug. 15, 1980, pp. 1612-1628.

62. Andersen, H. H.; Bak, J. F.; Knudsen, H.; and Nielsen, B. R.: Stopping Power of Al, Cu, Ag, and Au for MeV Hydrogen, Helium, and Lithium Ions Z_1^3 and Z_1^4 Proportional Deviations From the Bethe Formula. Phys. Rev. A, vol. 16, no. 5, Nov. 1977, pp. 1929-1940.

63. Khandelwal, G. S.: Stopping Power of K and L Electrons. Phys. Rev. A, vol. 26, no. 5, Nov. 1982, pp. 2983-2986.

64. Kahn, David: The Energy Loss of Protons in Metallic Foils and Mica. Phys. Rev., second ser., vol. 90, no. 4, May 15, 1953, pp. 503-509.

65. Neilsen, L. P.: Energy Loss and Straggling of Protons and Deuterons. Mat.-Fys. Medd. - K. Dan. Vidensk. Selsk., vol. 33, no. 6, 1961.

66. Leminens, E.; Fontell, A.; and Bister, M.: Stopping Power of Al, Zn and In for 0.6-2.5 MeV Protons. Ann. Acad. Sci. Fenn., no. 287, 1968.

67. Nakata, Hiroshi: Analysis of Energy-Loss Data for 0.2-0.5 MeV/amu p, α, and N in Se. Phys. Rev. B, vol. 3, no. 9, May 1, 1971, pp. 2847-2851.

68. Sorensen, H.; and Andersen, H. H.: Stopping Power of Al, Cu, Ag, Au, Pb, and U for 5-18-MeV Protons and Deuterons. Phys. Rev. B, vol. 8, no. 5, Sept. 1, 1973, pp. 1854-1863.

SYMBOLS

a_o	Bohr's radius
C	shell correction
c	velocity of light in vacuum
$\vec{D}(t)$	electric displacement vector
E	system excitation energy
$\vec{E}(t)$	electric field vector
E_n	eigenvalue of nth state
$E_{lr,corr}$	long-range correlation energy
e	magnitude of electron charge
$F(\omega)$	accumulated oscillator strength with angular frequency below ω
$F_D(\omega)$	Dalgarno sum
$f(\omega), f_n$	optical oscillator strength
$f_H(\omega)$	optical oscillator strength of hydrogen atom
$f_p(\omega)$	plasma oscillator strength of hydrogen atom
$g(\tau)$	polarization response
H	Hamiltonian operator
h	Planck's constant
$\hbar$	$h/2\pi$
I	mean excitation energy
I_{at}	atomic mean excitation energy
I_B	molecular mean excitation energy for Bragg's rule with neutral atoms
I_C	mean excitation energy of covalent bonded molecule
I_{IB}	molecular mean excitation energy for Bragg's rule with partially ionic atoms
I_j	mean excitation energy of system j
k	wave number of ejected electron
LPM	local plasma model

$L(m)$	mth moment of log mean excitation energy
ℓ	individual electron orbital angular momentum quantum number
m	electron mass
n	density of atoms
n_j	stochiometric coefficient
R	Rydberg's constant
R_{AB}	internuclear distance in molecule composed of atoms A and B
$\vec{r}, \vec{r}_i$	electron position vector
r_s	radius of Wigner-Seitz sphere
S	stopping power
$S(m)$	mth moment of oscillator strengths
t	time
v	ion velocity
Z_1	ion charge number
Z_2, Z_j	atomic number
β	ratio of ion velocity to velocity of light
γ	plasma frequency shift
Δ	straggling parameter
δ	polarization correction
δ_{ij}	chemical bond shift in mean excitation energy
$\varepsilon(\omega)$	dielectric function
λ_s	average electron separation
$\rho, \rho_i(\vec{r})$	electron density
$\rho_H(\vec{r})$	electron density in hydrogen atom
$\rho_{H_2}(\vec{r})$	electron density in hydrogen molecule
χ	screening parameter
ψ_o	ground state electronic wave function
ω, ω_n	angular frequency of oscillator

ω_p classical plasma frequency

$\langle\ \rangle$ averaged value

An arrow over a symbol denotes a vector. A prime over a symbol denotes a variable of integration.

TABLE I.- HYDROGEN MEAN EXCITATION ENERGY FOR STOPPING POWER

Chemical species	Hydrogen mean excitation energy, eV, for stopping power for -			
	Quantum model	Oscillator strength distribution	Local plasma model (a)	Experiment
H	14.99[b]		14.69	
H_2	18.2[c]	18.4[d]	18.9	18.5 ± 0.5[e]

[a]Using Pines correction.
[b]Using oscillator strengths of equation (25).
[c]Reference 14.
[d]Reference 37.
[e]Reference 40.

TABLE II.- HYDROGEN AND CARBON MOLECULAR PARAMETERS

Molecular parameter	H-H	H-C	C-H	C-C	C=C	C≡C	H-C benzene	C-H benzene	CC benzene	CC graphite
R_{AB}, a_o	1.40	2.08	2.08	2.94	2.52	2.28	2.02	2.02	2.64	2.68
δ	.261	.432	.044	.062	.087	.105	.453	.045	.079	.076

TABLE III.- MOLECULAR MEAN EXCITATION ENERGY

Chemical species	Molecular mean excitation energy, eV, for -		
	Present theory	Experimental empirical	Bragg's rule
CH_4	44.7	42.8	35.1
$(CH_2)_x$	55.0	53.4	43.5
C_6H_6	60.6	61.4 ± 1.9	50.6
H_2	18.9	18.5 ± 0.5	15.0
Graphite	76.1	78.5 ± 1.5	62.0

TABLE IV.- MOLECULAR MEAN EXCITATION ENERGIES FOR COVALENT GASES

Chemical species	R_{AB}, a_o	I, eV (a)	I, eV (b)
H_2	1.40	18.9	19.2 ± 0.4[c]
N_2	2.08	85.0	82.0 ± 1.6[c]
O_2	2.34	99.6	95 ± 1.9[c]
F_2	2.67	114.2	115 ± 10
Cl_2	3.76	170.8	171 ± 14

[a]Local plasma model.
[b]Reference 40.
[c]These values are strongly influenced by reference 11.

TABLE V.- MEAN EXCITATION ENERGIES FOR COVALENT-BONDED CRYSTALS

Chemical species	R_{AB}, a_o	I, eV (a)	I, eV (b)
B (tetragonal)	3.06	67.3	76 ± 7.6
C (diamond)	2.94	75.3	
C (graphite)	2.68	76.1	78 ± 2.3
Si (diamond)	4.42	151.0	173 ± 4
P (black)	4.16	155.7	181 ± 14[c]
S (rhombic)	3.85	162.7	190 ± 15[c]

[a]Local plasma model.
[b]Reference 40.
[c]Unspecified allotropic form.

TABLE VI.- IONIC-BOND PARAMETERS

Chemical species	R_{AB}, a_o	p	I_c, eV	I_{IB}, eV	I_B, eV	I, eV
HF	1.72	0.50	97.6	91.7	91.0	96.4
LiH	3.85	.25	27.8	25.2	25.9	26.7
LiF	3.85	.90	83.4	92.6	81.6	93.6

TABLE VII.- MEAN EXCITATION ENERGIES OF IONIC CRYSTALS

Chemical species	R_{AB}, a_o	p	I, eV (a)	I, eV (b)
LiF	3.80	0.90	92.8	94 ± 8
LiCℓ	4.86	.73	139.1	144 ± 12
NaF	4.37	.91[c]	131.5	147 ± 12
NaCℓ	5.31	.75	159.1	181 ± 14

[a]Local plasma model.
[b]Reference 40.
[c]Pauling partial ionic character function.

TABLE VIII.- METALLIC PARAMETERS FOR SELECTED METALS OF FIRST TWO ROWS

Chemical species	I_{at}, eV (a)	r_s, a_o	I, eV (b)	I, eV (c)
Lithium	34.0	3.260	45	41.5 ± 3.7
Beryllium	38.6	2.375	60	63.7 ± 3.2
Sodium	123.6	3.99	140	162 ± 8
Magnesium	121.2	3.34	144	164 ± 8
Aluminum	124.3	2.991	149	166 ± 3

[a]Reference 6.
[b]Wigner-Seitz model.
[c]Reference 40.

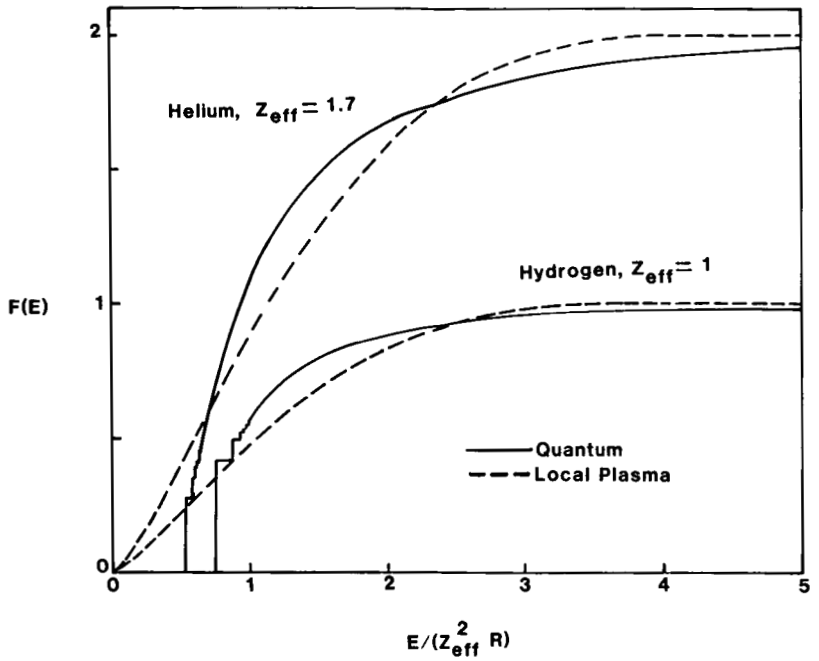

Figure 1.- Cumulative oscillator strength distribution for atomic hydrogen and helium.

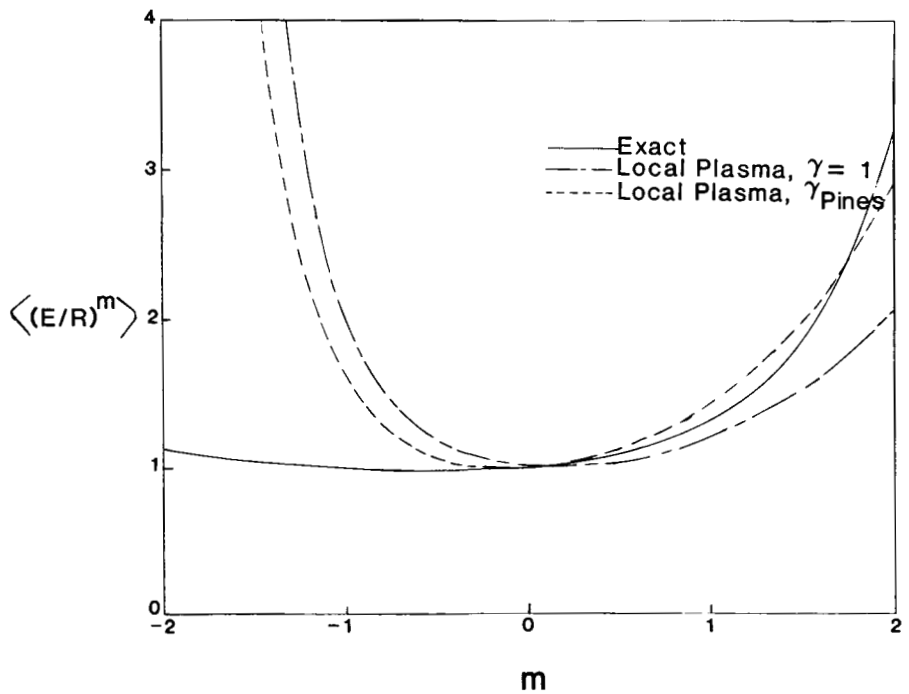

Figure 2.- Moments of oscillator strengths of hydrogen atom.

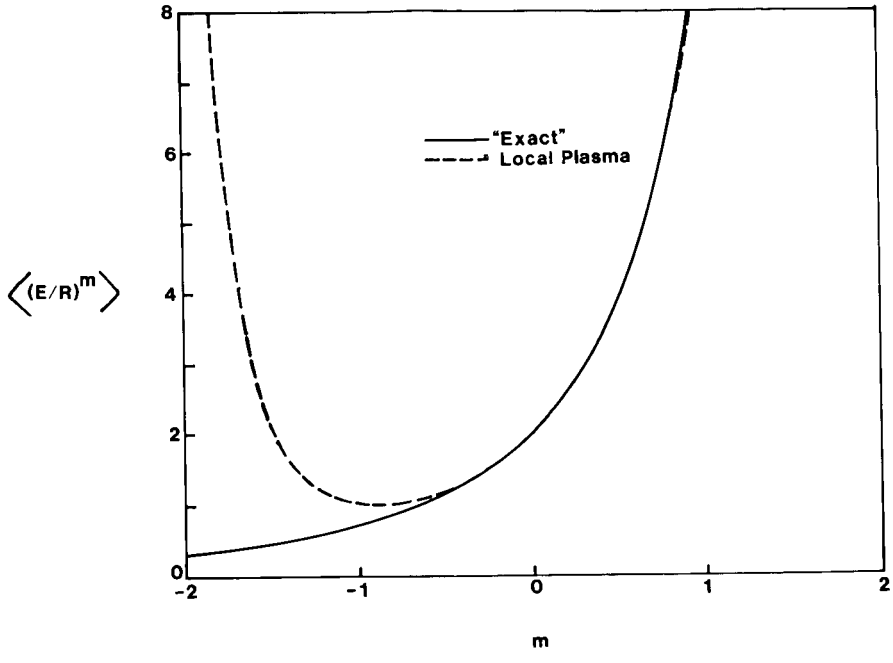

Figure 3.- Moments of oscillator strengths of helium atom according to quantum oscillator strengths using screened wave functions. $Z_{eff} = 1.7$.

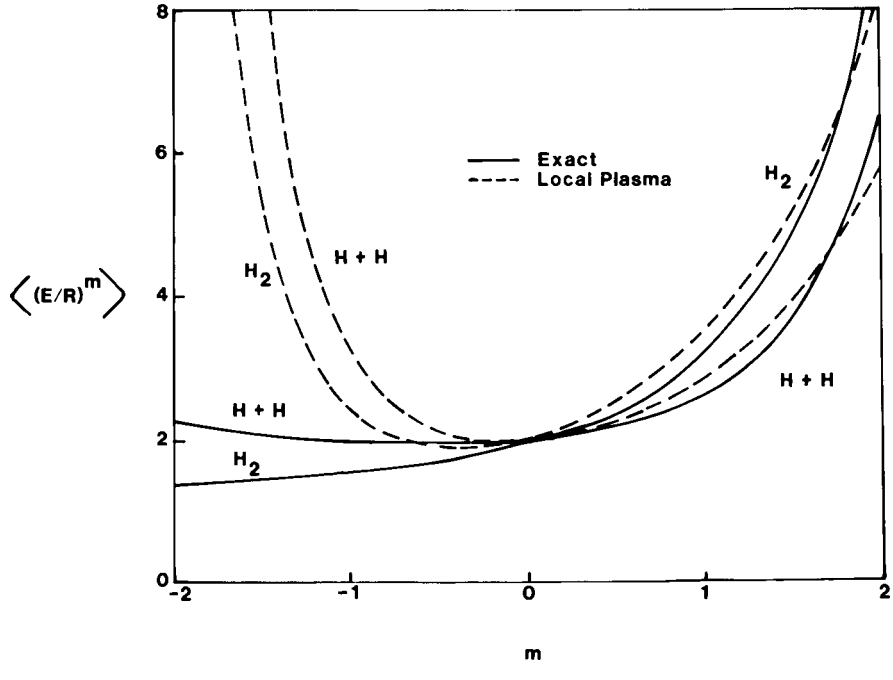

Figure 4.- Moments of oscillator strengths of hydrogen molecule for several models.

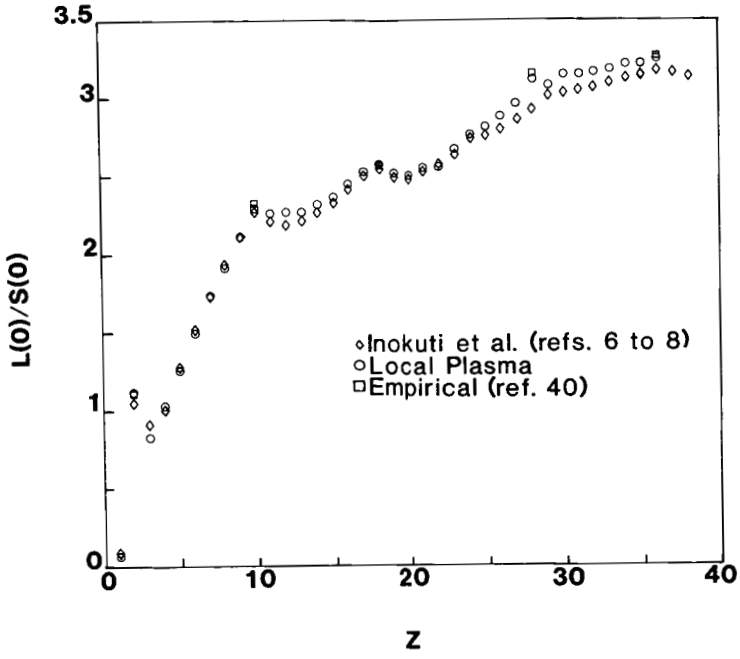

Figure 5.- Comparison of atomic mean excitation energies according to quantum calculations of Inokuti et al. and local plasma model. Empirical values are from reference 40.

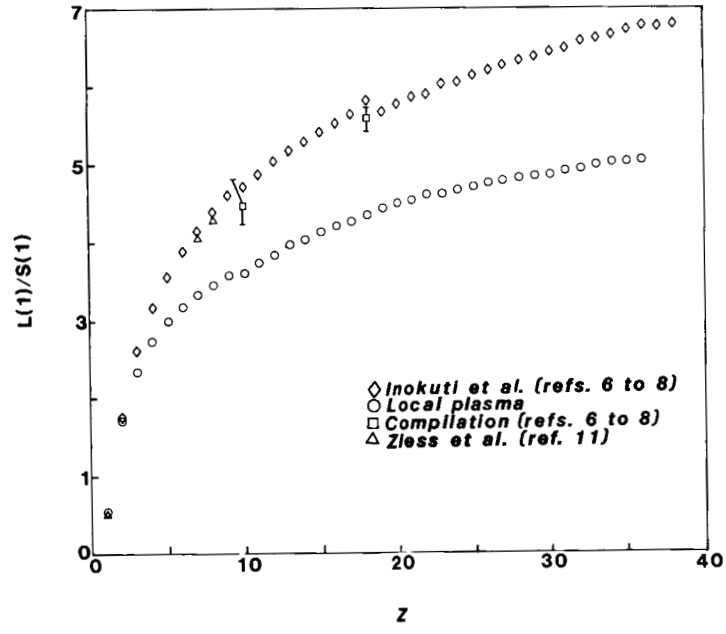

Figure 6.- Comparison of atomic straggling parameters according to quantum calculations of Inokuti et al. (refs. 6 to 8) and local plasma model.

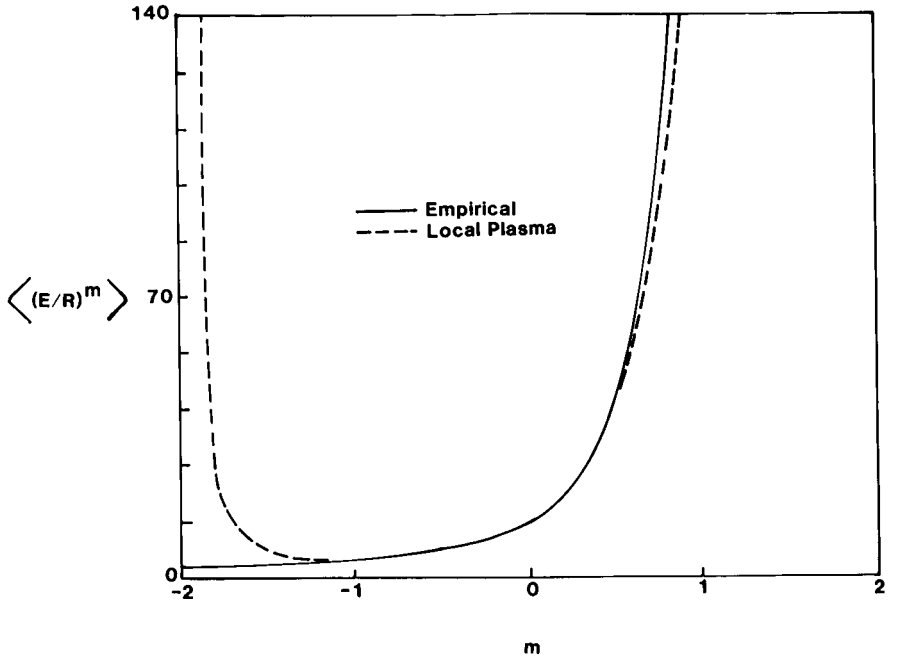

Figure 7.- Moments of oscillator strengths from empirical values of reference 49 compared with local plasma model using Gordon-Kim molecular model densities.

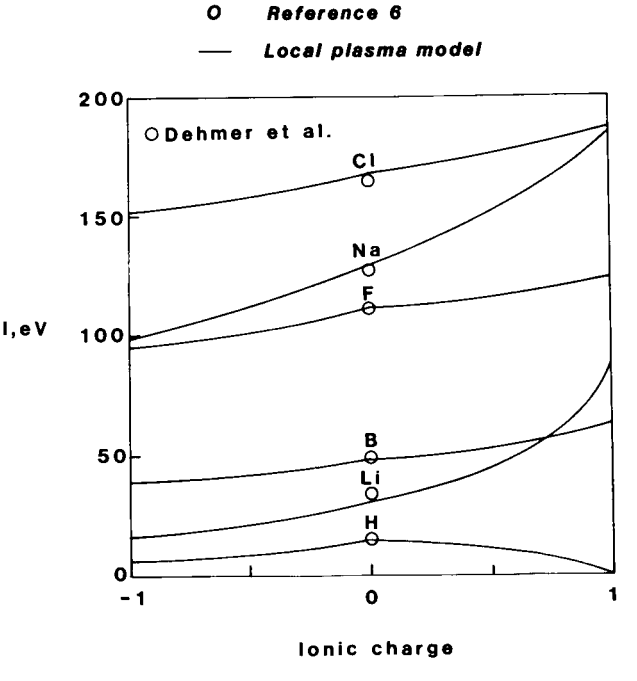

Figure 8.- Mean excitation energies for partially ionic atoms.

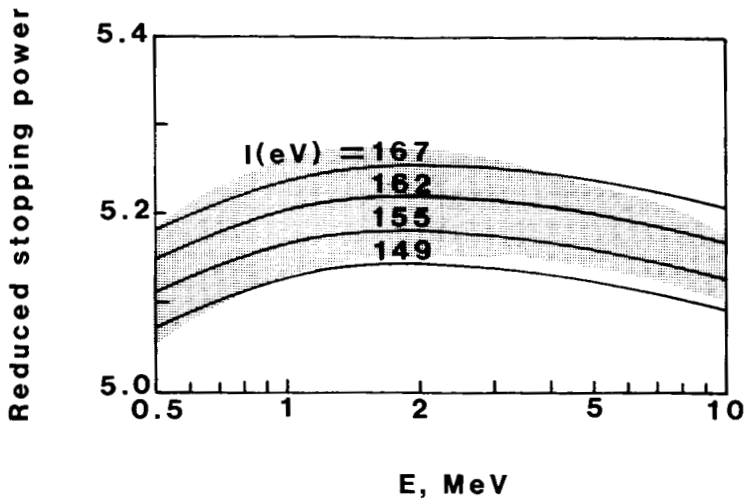

Figure 9.- Comparisons of reduced stopping power for aluminum for several mean excitation energies with range of experimental data. (See refs. 60 and 62 to 66.) Shaded area is band of experimental data.

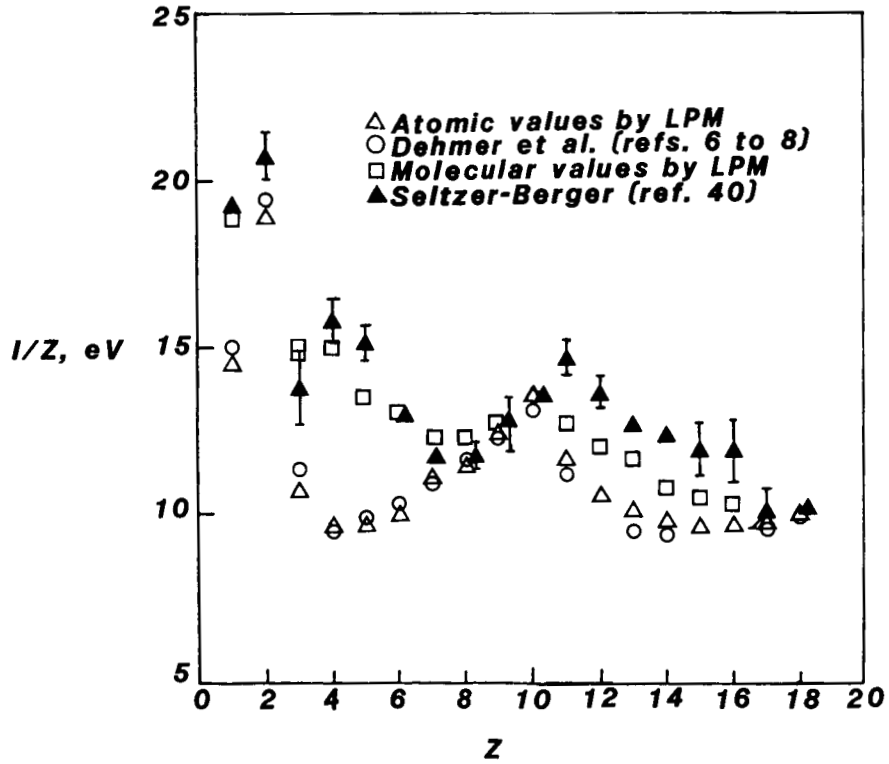

Figure 10.- Mean excitation energies for atoms, molecules, solids, and metals. Specific data taken from tables III to V and table VIII.

1. Report No.	2. Government Accession No.	3. Recipient's Catalog No.
NASA TP-2271		

4. Title and Subtitle	5. Report Date
MEAN EXCITATION ENERGIES FOR STOPPING POWERS IN VARIOUS MATERIALS USING LOCAL PLASMA OSCILLATOR STRENGTHS	March 1984
	6. Performing Organization Code 506-55-23-03

7. Author(s)	8. Performing Organization Report No.
John W. Wilson, Y. J. Xu, Efstathios Kamaratos, and C. K. Chang	L-15731
	10. Work Unit No.

9. Performing Organization Name and Address	11. Contract or Grant No.
NASA Langley Research Center Hampton, VA 23665	
	13. Type of Report and Period Covered Technical Paper

12. Sponsoring Agency Name and Address	14. Sponsoring Agency Code
National Aeronautics and Space Administration Washington, DC 20546	

15. Supplementary Notes

John W. Wilson: Langley Research Center, Hampton, Virginia.
Y. J. Xu: Old Dominion University, Norfolk, Virginia (NASA Grant NSG-1614).
E. Kamaratos and C. K. Chang: Christopher Newport College, Newport News, Virginia (NASA Cooperative Agreement NCC1-42).

16. Abstract

The basic model of Lindhard and Scharff, known as the local plasma model, is utilized to study the effects on stopping power of the chemical and physical state of the medium. Unlike previous work with the local plasma model, in which individual electron shifts in the plasma frequency were estimated empirically, the Pines correction derived for a degenerate Fermi gas is shown herein to provide a reasonable estimate, even on the atomic scale. Thus, the model is moved to a complete theoretical base requiring no empirical adjustments, as characteristic of past applications. The principal remaining error is in the overestimation of the low-energy absorption properties that are characteristic of the plasma model in the region of the atomic discrete spectrum, although higher-energy phenomena are accurately represented, and even excitation-to-ionization ratios are given to fair accuracy. Mean excitation energies for covalent-bonded gases and solids, for ionic gases and crystals, and for metals are calculated using first-order models of the bonded states, for which reasonable agreement with the recently evaluated data of Seltzer and Berger is obtained. Hence, the methods described herein allow reasonable estimates of mean excitation energy for any physical-chemical combination of material media for stopping-power applications.

17. Key Words (Suggested by Author(s))	18. Distribution Statement
Stopping power Molecules Protons	Unclassified - Unlimited Subject Category 93

19. Security Classif. (of this report)	20. Security Classif. (of this page)	21. No. of Pages	22. Price
Unclassified	Unclassified	36	A03

For sale by the National Technical Information Service, Springfield, Virginia 22161

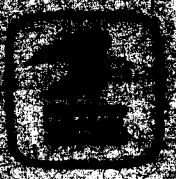

3 2 1U,J, 840315 S00161DS
DEPT OF THE AIR FORCE
ARNOLD ENG DEVELOPMENT CENTER(AFSC)
ATIN: LIBRARY/DOCUMENTS
ARNOLD AF STA TN 37389